

Field monitoring of the train-induced hanger vibration in a high-speed railway steel arch bridge

Youliang Ding¹, Yonghui An^{*2} and Chao Wang¹

¹*School of Civil Engineering, Key Laboratory of C&PC Structures of the Ministry of Education, Southeast University, Nanjing 210096, China*

²*Department of Civil Engineering, State Key Laboratory of Coastal and Offshore Engineering, Dalian University of Technology, Dalian 116023, China*

(Received November 23, 2015, Revised April 16, 2016, Accepted April 19, 2016)

Abstract. Studies on dynamic characteristics of the hanger vibration using field monitoring data are important for the design and evaluation of high-speed railway truss arch bridges. This paper presents an analysis of the hanger's dynamic displacement responses based on field monitoring of Dashengguan Yangtze River Bridge, which is a high-speed railway truss arch bridge with the longest span throughout the world. The three vibration parameters, i.e., dynamic displacement amplitude, dynamic load factor and vibration amplitude, are selected to investigate the hanger's vibration characteristics in each railway load case including the probability statistical characteristics and coupled vibration characteristics. The influences of carriageway and carriage number on the hanger's vibration characteristics are further investigated. The results indicate that: (1) All the eight railway load cases can be successfully identified according to the relationship of responses from strain sensors and accelerometers in the structural health monitoring system. (2) The hanger's three vibration parameters in each load case in the longitudinal and transverse directions have obvious probabilistic characteristics. However, they fall into different distribution functions. (3) There is good correlation between the hanger's longitudinal/transverse dynamic displacement and the main girder's transverse dynamic displacement in each load case, and their relationships are shown in the hysteresis curves. (4) Influences of the carriageway and carriage number on the hanger's three parameters are different in both longitudinal and transverse directions; while the influence on any of the three parameters presents an obvious statistical trend. The present paper lays a good foundation for the further analysis of train-induced hanger vibration and control.

Keywords: steel truss arch bridge; railway; hanger; dynamic displacement; static displacement; dynamic load factor; correlation; monitoring

1. Introduction

A lot of long-span bridges have been built for the purpose of increasing the transport capacity, strengthening the region connection, etc. Large-scale bridges play a vital role in modern economies (An *et al.* 2015); however, they are suffering from structural condition deterioration because they are exposed to environmental conditions and external dynamic loads (Li *et al.* 2015a),

*Corresponding author, Associate Professor, E-mail: anyh@dlut.edu.cn

and their failure will cause severe loss for society and economy. As a result, structural health monitoring (SHM) has become an important research topic for structural safety evaluation and continuous condition assessment (Li *et al.* 2015a), and the SHM system gets widely application (Li *et al.* 2015b) in large-scale bridges. Structural vibration responses are widely used for condition assessment with damage diagnosis methods (An *et al.* 2014, An *et al.* 2016), and the diagnosis results can also support SHM (Li *et al.* 2015c) for structure abnormality alarming. Zhou *et al.* (2013) reviews the SHM benchmark studies, in which the physical structure, the numerical study, the scaled laboratorial model experiment and latest developments on the application of SHM techniques are reviewed. It's necessary to analyze the bridge characteristics based on the long-term monitoring data from the SHM system.

The long-term monitoring data from SHM system are analyzed to obtain the structural damage and abnormality which can provide guidance for the further maintenance, reinforcement and even the future design. Many studies based on bridge field monitoring data have been conducted. Saito and Sakata (1999) collected structural characteristics and natural wind characteristics data from both field measurement and wind tunnel test for a long-span box girder bridge to evaluate its aerodynamic stability. Feng *et al.* (2005) assessed global structural conditions and identified the damage location in highway bridges for further bridge damage assessment based on traffic-induced and ground-motion-induced vibration data respectively. Ni *et al.* (2006) utilized long-term monitoring data from a suspension bridge to assess bridge fatigue life based on a statistical probability distribution method. Ni *et al.* (2007) established a normal correlation pattern based on the long-term monitoring data of the bridge temperature and expansion joint displacement, which can predict the expansion joint displacements and estimate the service life and the interval for replacement of expansion joints. Pinkaew and Senjuntichai (2009) concerned the fatigue damage caused by train-induced dynamic strains in a railway truss bridge and evaluated the fatigue damage risk of different bridge members. Bayraktar *et al.* (2010) got test result from the measurement of a highway bridge in order to analyze traffic-induced vibration and the bridge's dynamic characteristics, and they established and updated the finite element (FE) model of the bridge according to the experimental data. Ye *et al.* (2012) developed a monitoring-based method for steel bridges' fatigue life assessment based on long-term monitoring strain data, and railway traffic, highway traffic and typhoon effects are accounted in the statistical analysis of the stress spectra for formulating a standard daily stress spectrum. Norouzi *et al.* (2013) proposed a methodology which is used to find abnormal performance of the bridge by establishing a simple data model based on the long-term monitoring data patterns. Chiu *et al.* (2014) did in-situ experiments and collected long-term monitoring data for dynamic behavior analysis in real bridges, and numerical models were constructed combined with in-situ experiments for a better bridge safety evaluation and life-cycle management. Liu *et al.* (2014) recommended a method to calculate the localized reliability around an embedded sensor based on a long-term SHM system monitoring data, and this method can be used for further structural analysis and maintenance. Acampora *et al.* (2014) got vibration data of the full-scale cable and applied it in the identification of the total stiffness matrix and total damping matrix. The back-calculated drag coefficient from the damping matrix agrees well with the measured drag coefficient from the wind tunnel test.

With elegant appearance and good mechanical properties, more and more arch bridges are built nowadays. The hangers are the main connection components between the arch and deck, and damage of hangers will cause severe influence. The vibration of hangers induced by ambient excitation may result in their damage or fatigue accumulation, many cases about large vibration of the arch bridge hangers can be listed (Chen *et al.* 2011); for example, Dong Ping Bridge, a steel

arch bridge, was attacked by typhoon on August 4, 2006 and more than 20 hangers had excessive vibration simultaneously. Many other similar cases can be found in arch bridges around the world, and there is hidden danger which is harmful to the long-term performance of bridges. Moreover, the traffic loads may bring great impact in short times, which can affect the hangers' vibration significantly. Therefore, it is essential to study the hangers' vibration caused by vehicle-bridge interaction. There has been much research on the hangers' vibration induced by vehicle-bridge interaction in recent years. Chatterjee and Datta (1995) used a mixed method, which combined the advantages of continuum and lumped mass methods, to analyze the dynamic characteristics of a bridge with a relatively rigid arch supporting a flexible deck under a single moving load. Ju and Lin (2003) analyzed the vibration characteristics of a steel arch bridge considering three-dimensional train-bridge interaction under a high-speed train, and two simple resonance criteria for the arch bridge and high-speed train resonance effect prediction are recommended and validated by FE analysis. Malm and Andersson (2006) analyzed the hangers' field measurements in a tied arch bridge and the corresponding FE model to investigate the hangers' vibration induced by the train for fatigue evaluation of the bridge. Zeng and Tan (2012) discussed the method to compute the hangers' fatigue reliability under vehicle loads based on the accurate analysis of vehicle load spectrum. Shao *et al.* (2015) studied vehicle induced dynamic internal force of hangers in a half-through arch bridge; they used both measurement data and numerical method for hanger system's fatigue analysis and service life evaluation in view of vehicle-bridge interaction and road surface roughness. To sum up, many great vibration analysis methods for the arch bridge hangers have been proposed. However, little research about hanger vibration of the high-speed railway arch bridges based on the long-term monitoring data has been found. Field measurement method is the most accurate way to obtain bridge behavior, and the vibration characteristics of hangers can be estimated accurately based on the monitoring data.

Dashengguan Yangtze River Bridge, the first 6-track railway arch bridge in the world, the high-speed railway bridge with the highest loading capacity in the world, and the longest high-speed railway arch bridge with a continuous arch of the design speed of 300km/h in the world, is selected as the research object to study the hangers' vibration. The bridge is a multi-span continuous arch bridge with a total length of 1615m. It consists of six tracks that include two lines for the Beijing-Shanghai High Speed Railway, two lines for the Shanghai-Wuhan-Chengdu Railway and two lines for the Nanjing Metro, and the main span is a continuous steel truss arch with 21 hangers (Wang *et al.* 2015). The transverse and longitudinal vibration data of a hanger is collected by sensors in the SHM system. Ding *et al.* (2015) preliminarily discussed the probability statistics of a hanger's dynamic displacement amplitudes and their relationship with the main girder of Dashengguan Yangtze River Bridge based on the long-term monitoring data.

In this paper, the vibration data of hangers collected from SHM system is studied with consideration of vehicle-bridge interaction based on the three parameters, i.e., the dynamic displacement, the dynamic load factor and the vibration amplitude. For this purpose, the remainder of this paper is organized as follows: section 2 shows the dynamic displacement monitoring of a selected hanger in the bridge; section 3 provides the characteristic analysis of train-induced dynamic displacements; and finally section 4 gives the conclusions.

2. Field monitoring of train-induced hanger's dynamic displacements

As shown in Fig. 1, the Dashengguan Yangtze River Bridge is a double continuous steel truss

girder and a continuous steel truss arch bridge with a main span arrangement of 108 m+192 m+336 m+336 m+192 m+108 m.

2.1 Dynamic displacement monitoring method

The SHM system has been set up for the Dashengguan Yangtze River Bridge, in which some velocimeters have been installed on the hangers for the long-term monitoring of train-induced hanger's dynamic responses. In order to monitor the 1# hanger's dynamic displacement responses, two velocimeters are installed on the 1# hanger at the girder's section 1-1 in the transverse and longitudinal directions respectively (Fig. 1). The detailed locations of the two sensors are shown in Fig. 2, in which the sensor Z1 is the velocimeter to measure the longitudinal responses and the sensor Z2 is the velocimeter to measure the transverse responses. The sampling frequency is 200 Hz. As shown in Fig. 2, dynamic strain sensors Y1 and Y2 (Fig. 2) are installed on the cross girders of downstream side and upstream side at the section 1-1 (Fig. 1) of the bridge respectively; accelerometers J1 and J2 are installed on the girder, above the 2# pier and 20# pier, respectively.

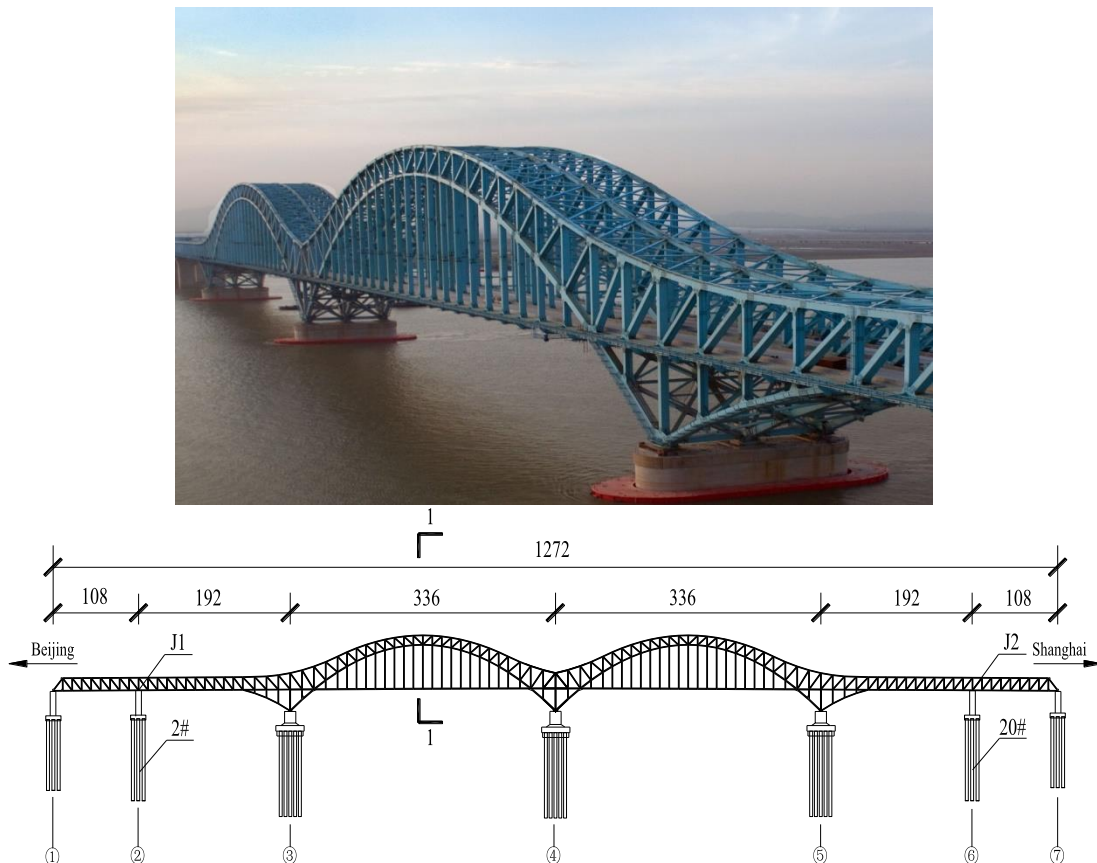


Fig. 1 The Dashengguan Yangtze River Bridge

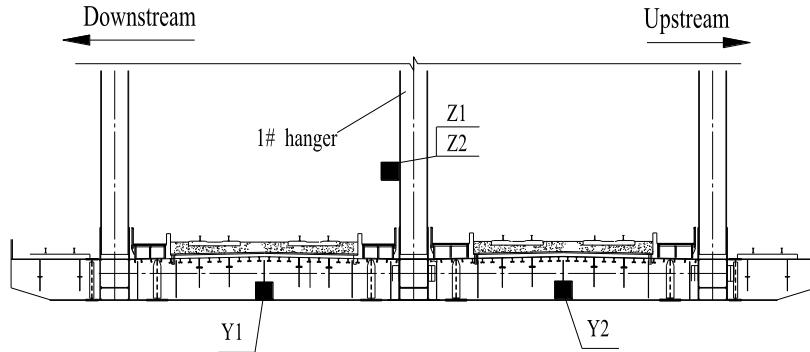


Fig. 2 The detailed sensor layout on the section 1-1

Here the dynamic displacement responses are obtained by the integral of vibration velocity responses. To improve the integral accuracy, Romberg integral (Katani and Shahmorad 2012) is employed as follows due to its simple procedure and the high accuracy:

$$T_{2n} = \frac{1}{2} \left(T_n + h \sum_{k=0}^{n-1} f(x_{k+1}) \right) \tag{1}$$

$$S_n = T_{2n} + 1/3(T_{2n} - T_n) \tag{2}$$

$$C_n = S_{2n} + 1/15(S_{2n} - S_n) \tag{3}$$

$$R_n = C_{2n} + 1/63(C_{2n} - C_n) \tag{4}$$

where $n = 0, 1, 2, 3, \dots$; h is the derivative of sampling frequency; x_{k+1} is the time of the $(k+1)$ th data point; $f(x_{k+1})$ is the velocity at time point x_{k+1} ; T_n , S_n , C_n and R_n are the n th data point of the dynamic displacement obtained based on compound trapezoid formula, compound Simpson formula, compound Cotes formula and Romberg integral, respectively; Eqs. (1)-(3) are the compound trapezoid formula, compound Simpson formula and compound Cotes formula respectively; Romberg integral has an advantage of high accuracy and quick convergence because it uses compound trapezoid formula which is very simple in the procedure.

2.2 Dynamic displacement monitoring results

Different railway load cases have different influences on the hanger's dynamic displacement monitoring results, so it is very important to investigate these influences through the fine analysis of different load cases. Thus, according to the carriageway and carriage number, this section conducts the fine analysis of the 1# hanger' dynamic displacement monitoring results based on 8 railway load cases. The 8 railway load cases are summarized in Table 1 and Fig. 3 for a simple description. Note that only the cases that one train runs through the bridge are considered in this work. The cases that multiple trains run through the bridge at the same time are not discussed here due to the complex mechanical characteristics. Considering there is no any sensor or instrument which is used for distinguishing the load cases in the SHM system of Dashengguan Yangtse River

Bridge, eight load cases (Table 1) can be identified by the relationship analysis of responses from the strain sensors and the accelerometers installed in the SHM system.

The proposed load case identification method is introduced in detail as follows:

(1) Figs. 4 and 5 show the strain responses from sensors Y1 and Y2 when the train runs on the downstream side and upstream side respectively. The response measured from sensor Y1 has a larger change than that from sensor Y2 when the train is running on the downstream side; the response measured from sensor Y2 has a larger change than that from sensor Y1 when the train is running on the upstream side. According to this rule, the side that the train runs on can be determined.

(2) Nine extreme points will be produced by the 9 pairs of wheels when a 8-carriages train runs through a strain sensor; 17 extreme points will be produced by the 17 pairs of wheels when a 16-carriage train runs through a strain sensor. As shown in Fig. 6, the carriage number can be determined according to this rule.

(3) As shown in Fig. 7, when the train runs from Beijing to Shanghai, the extreme point of the acceleration response from the accelerometer J1 (2# pier) presents earlier than that in the acceleration response from the accelerometer J2 (20# pier); vice versa. As a result, the driving direction can be determined. Finally the railway load case can be identified accurately.

Table 1 The 8 load cases

Case number	Descriptions of the load case
Case 1	A 8-carriage train runs on the downstream side from Shanghai to Beijing
Case 2	A 8-carriage train runs on the downstream side from Beijing to Shanghai
Case 3	A 16-carriage train runs on the downstream side from Shanghai to Beijing
Case 4	A 16-carriage train runs on the downstream side from Beijing to Shanghai
Case 5	A 8-carriage train runs on the upstream side from Shanghai to Beijing
Case 6	A 8-carriage train runs on the upstream side from Beijing to Shanghai
Case 7	A 16-carriage train runs on the upstream side from Shanghai to Beijing
Case 8	A 16-carriage train runs on the upstream side from Beijing to Shanghai

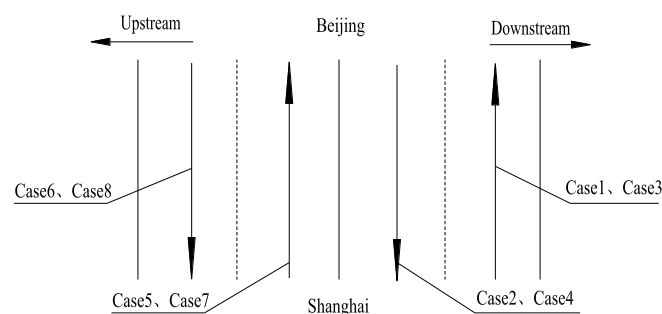


Fig. 3 A simple description of 8 load cases

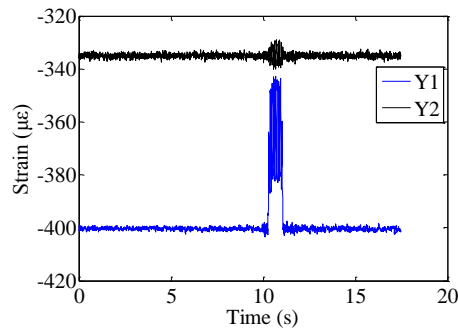


Fig. 4 The strain time histories of the cross girder when a train runs on the downstream side from sensor Y1 and Y2

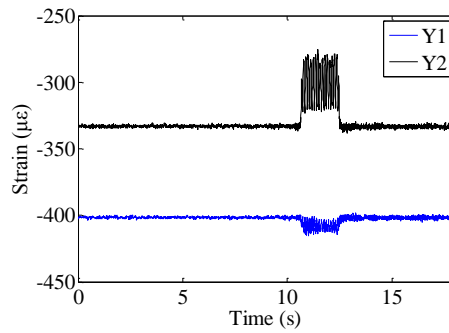


Fig. 5 The strain time histories of the cross girder when a train runs on the upstream side from sensor Y1 and Y2

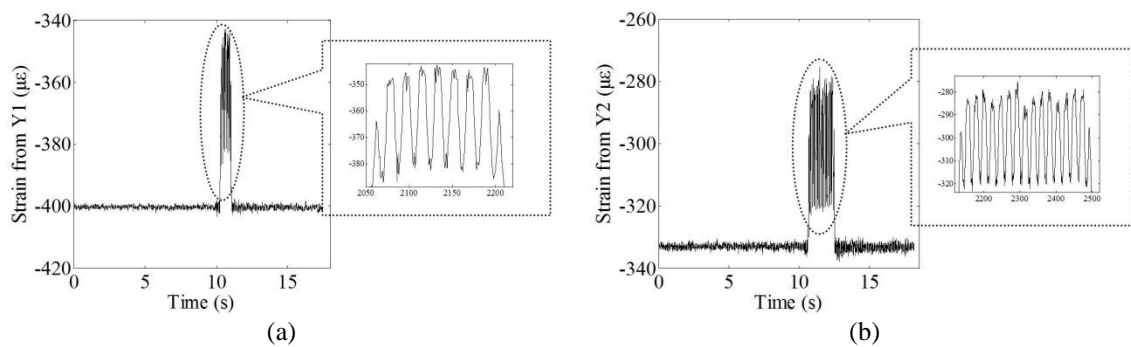


Fig. 6 The extreme points when the trains with different carriage numbers run through the bridge: (a) a 8-carriage train and (b) a 16-carriage train

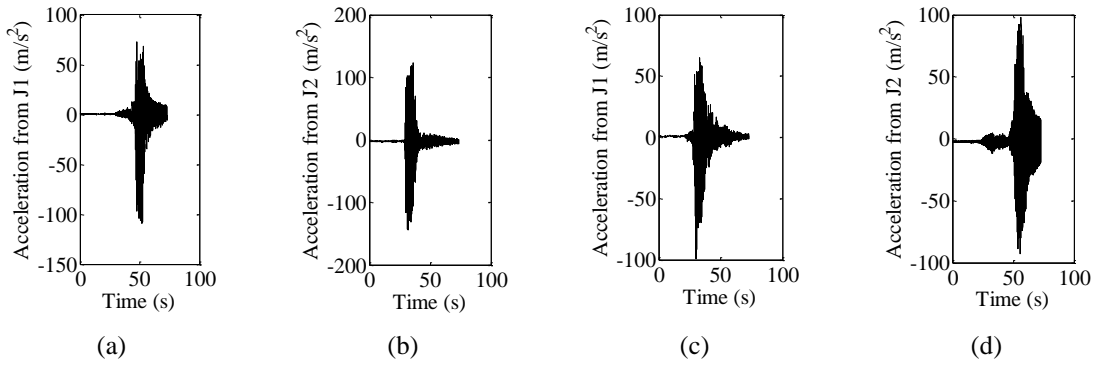


Fig. 7 Accelerations from the accelerometers J1 and J2: (a) acceleration from the sensor J1 when the train runs from Shanghai to Beijing, (b) acceleration from the sensor J2 when the train runs from Shanghai to Beijing, (c) acceleration from the sensor J1 when the train runs from Beijing to Shanghai and (d) acceleration from the sensor J2 when the train runs from Beijing to Shanghai

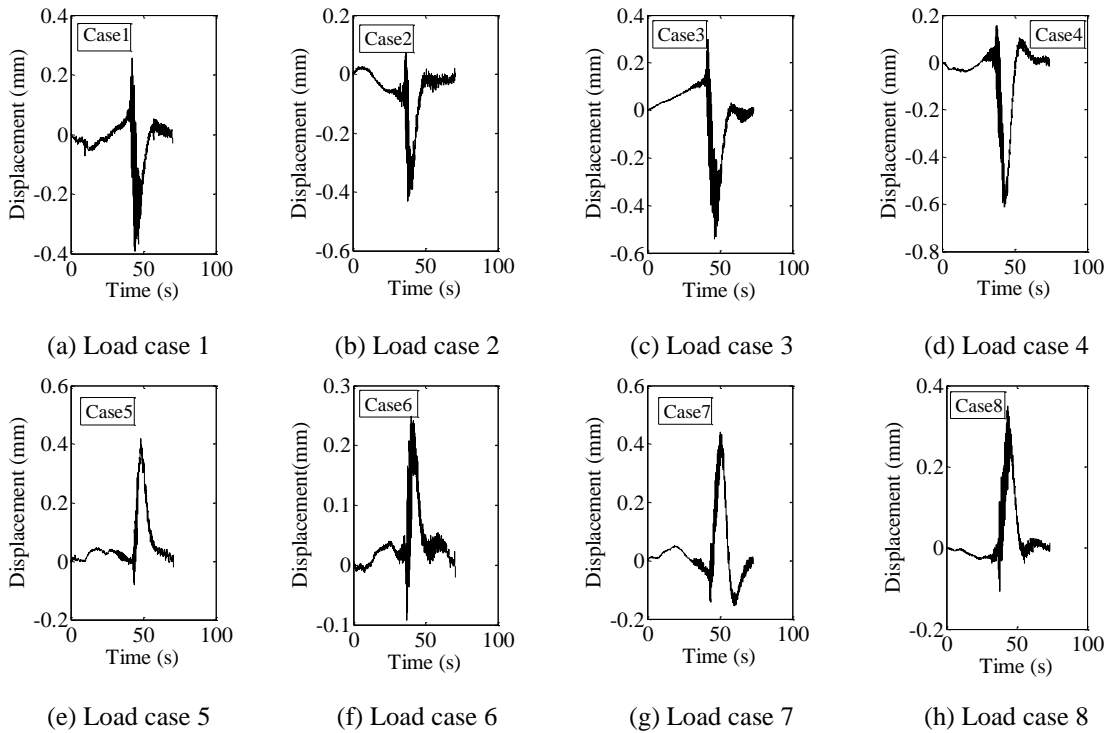


Fig. 8 Longitudinal dynamic displacement monitoring results of the 1# hanger for load cases 1~8 when a train runs through the bridge

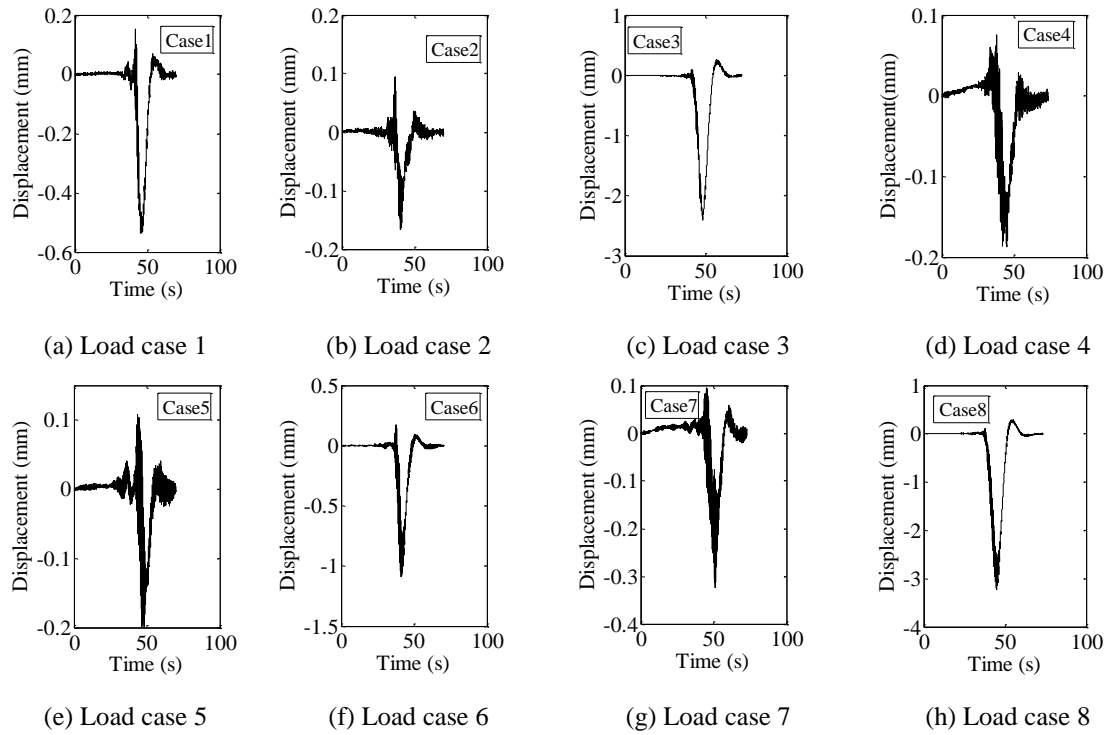


Fig. 9 Transverse dynamic displacement monitoring results of the 1# hanger for load cases 1~8 when a train runs through the bridge

Figs. 8 and 9 show the longitudinal and transverse dynamic displacement monitoring results of the 1# hanger for each load case when a train runs through the bridge. It can be seen from the figures that: all the dynamic displacement monitoring results are unimodal curves, which indicates that the time-varied characteristics of the hanger's longitudinal and transverse dynamic displacement are required to be noted. Moreover, there is a big difference in dynamic displacement amplitudes of different load cases and the dynamic displacement amplitude is influenced by the carriageway and carriage number.

The static displacement time history and vibration amplitude time history are further obtained from the dynamic displacement time history based on the wavelet filtering method. Taking the load case 1 for example, Figs. 10 and 11 show the 1# hanger's transverse static displacement time history and vibration amplitude time history when the high-speed train runs through the bridge. It can be seen from these figures that: The trend of the static displacement time history agrees well with that of the dynamic displacement time history; vibration amplitude time history varies with a small oscillations around the equilibrium position, and the oscillation amplitude has an obvious amplification when a train runs through the bridge. Hence, when a high-speed train runs through a bridge, the 1# hanger's dynamic displacement, static displacement and vibration amplitude time history in both longitudinal and transverse directions change obviously and can not be ignored, which also indicates that it is vital for hangers' fatigue to investigate the three monitoring parameters. Therefore, the long-term time-varied trends of the three monitoring parameters are required to be studied in this work. Influences of the carriageway and carriage number on three

selected parameters, i.e. dynamic displacement amplitude, dynamic load factor and vibration amplitude, are also studied quantitatively; in which dynamic displacement amplitude refers to the maximum absolute value of the displacement response, which is measured directly from a hanger or calculated based on the other kinds of responses measured from the hangers (for example the dynamic displacement response is obtained by the integral of velocity response of the hanger in this work); dynamic load factor refers to the ratio of a hanger's maximum dynamic displacement and maximum static displacement with the same traffic load, and the dynamic load factor can be obtained by (Shao *et al.* 2015)

$$DLF = \frac{R_{\text{dyn}}}{R_{\text{stat}}} \quad (5)$$

where R_{dyn} is the maximum absolute value of dynamic displacement of the hanger, i.e., the dynamic displacement amplitude, R_{stat} is the maximum absolute value of static displacement of the hanger. Vibration amplitude time history refers to the difference between the dynamic displacement amplitudes and the static displacement amplitudes, for example the vibration amplitude time history in Fig. 11 is the difference between the results in Figs. 9(a) and 10; vibration amplitude is the maximum absolute value of the vibration amplitude time history.

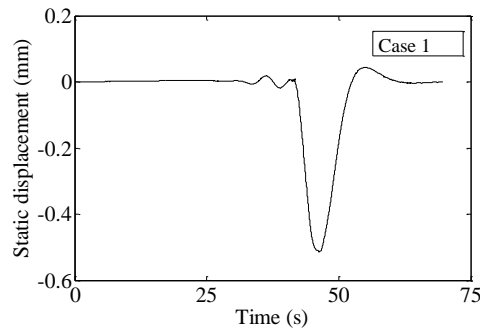


Fig. 10 The 1# hanger's transverse static displacement when a train runs through the bridge (load case 1)

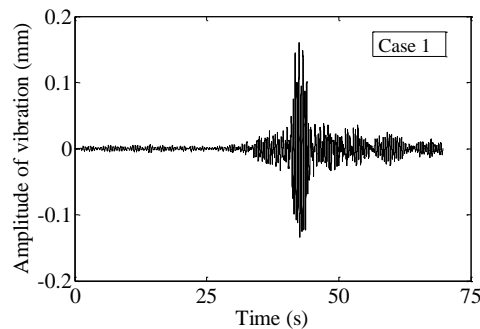


Fig. 11 The 1# hanger's transverse vibration amplitude time history when a train runs through the bridge (load case 1)

3. Characteristic analysis of train-induced dynamic displacements

3.1 Probability statistical characteristics

The probability statistical models of the three parameters, i.e., the hanger's longitudinal and transverse dynamic displacement amplitudes, dynamic load factors and vibration amplitudes in each load case when the train runs through the bridge in the year of 2013, are established in this section. Firstly, various probability density functions are used to compare the goodness of fit in each load case and the best probability density function is finally selected to describe the probability density distribution characteristics. The analysis of the three parameters is discussed as follows.

3.1.1 Amplitude of the dynamic displacement

Various probability density functions are used to compare the goodness of fit for the hanger's longitudinal dynamic displacement amplitudes in each load case. Finally the t location-scale distribution (The Math Works Inc 2010) is selected to describe the probability density distribution characteristics, and it is given by

$$f(x) = \frac{\Gamma\left(\frac{\nu+1}{2}\right)}{\sigma\sqrt{\nu\pi}\Gamma\left(\frac{\nu}{2}\right)} \left[\frac{\nu + \left(\frac{x-\mu}{\sigma}\right)^2}{\nu} \right]^{\left(\frac{\nu+1}{2}\right)} \quad (6)$$

where ν , μ , σ are shape parameter, location parameter and scale parameter respectively, and $\mu > 0$, $\sigma > 0$. If x has a t location-scale distribution, with parameters ν , μ and σ , then $\frac{x-\mu}{\sigma}$ has a t distribution with ν degrees of freedom. The parameters are determined by least square fitting of probability density of the hanger's longitudinal dynamic displacement amplitudes based on Eq. (6). Probability density fitting curves of the hanger's longitudinal dynamic displacement amplitudes in each load case based on one year's measured data are shown in Fig. 12; taking Case 1 in Fig. 12(a) for example, Fig. 12(c) shows the good agreement of the fitting curve and the original data. The corresponding estimated parameter values are shown in Table 2. It can be seen from the figure that:

- 1) Here the t location-scale distribution function can describe the probability density distribution characteristics well, which indicates that the 1# hanger's longitudinal dynamic displacement amplitudes in each load case have obvious probabilistic characteristics.
- 2) With the same load (the same carriage number), the longitudinal dynamic displacement amplitudes in the load cases close to the 1# hanger are slightly smaller than those in the load cases far away from the 1# hanger on the upstream side. However, the influences of the traveling direction of the train on 1# hanger's longitudinal dynamic displacement amplitudes in load cases 7 and 8 are slightly larger than the others.
- 3) In the same carriageway, the 1# hanger's longitudinal dynamic displacement amplitudes in the load cases with a 16-carriage train are greater than those in the load cases with a 8-carriage train.

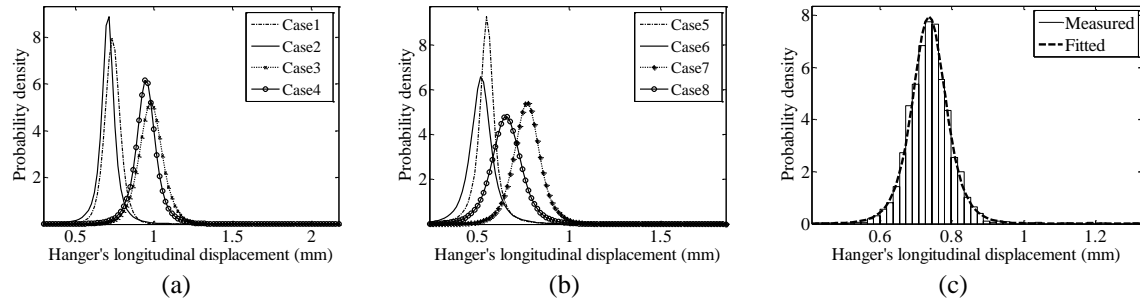


Fig. 12 Probability density fitting curves of the 1# hanger's longitudinal dynamic displacement amplitudes: (a) for load cases 1~4, (b) for load cases 5~8 and (c) the detailed figure including original data and the fitting curve for Case 1 in Fig. 12(a)

Table 2 Estimated parameter values of the t location-scale distribution function for the 1# hanger's longitudinal dynamic displacement amplitudes

Load case	1	2	3	4	5	6	7	8
μ	0.7365	0.7077	0.9803	0.9489	0.5506	8.6372	0.7700	12.643
σ	0.0476	0.0388	0.0737	0.0595	0.0380	1.7038	0.0695	2.2457
ν	4.9321	1.9650	5.9462	3.2325	1.9548	2.3430	4.3391	4.3392

Various probability density functions are used to compare the goodness of fit for the hanger's transverse dynamic displacement amplitudes in each load case. Finally the generalized extreme value distribution (Xia *et al.* 2012) is selected to describe the probability density distribution characteristics, and it is given by

$$f(T) = \frac{1}{a} \left[1 + r \left(\frac{T-b}{a} \right) \right]^{-1/r-1} \exp \left[- \left[1 + r \left(\frac{T-b}{a} \right) \right]^{-1/r} \right] \quad (7)$$

where r , b , a are the shape parameter, location parameter and scale parameter respectively. The parameters are determined by least square fitting of probability density of the hanger's transverse dynamic displacement amplitudes based on Eq. (7). Probability density fitting curves of the 1# hanger's transverse dynamic displacement amplitudes in each load case based on one year's measured data are shown in Fig. 13, and the corresponding estimated parameters are shown in Table 3. It can be seen from the figure that:

- 1) Here the generalized extreme value distribution function can describe the probability density distribution characteristics well, which indicates that the 1# hanger's transverse dynamic displacement amplitudes in each load case have obvious probabilistic characteristics.
- 2) With the same load, the transverse dynamic displacement amplitudes in the load cases close to the 1# hanger are much smaller than those in the load cases far away from the 1# hanger.

- 3) In the same carriageway, the influence of the load (i.e., the carriage number) on the 1# hanger's transverse dynamic displacement amplitudes is very small; the 1# hanger's transverse dynamic displacement amplitudes in load cases with a 16-carriage train are slightly larger than those in load cases with a 8-carriage train.

3.1.2 Vibration amplitude

Various probability density functions are used to compare the goodness of fit for the hanger's longitudinal and transverse vibration amplitudes in each load case. Finally the loglogistic distribution (Antony and Matthew 2002) is selected to describe the probability density distribution characteristics, and it is given by

$$f(x) = \frac{e^{-\frac{x-\mu}{\sigma}}}{\sigma \left(1 + e^{-\frac{x-\mu}{\sigma}}\right)^2} \tag{8}$$

where μ and σ are the parameters about location parameter and scale parameter respectively, and $\sigma > 0$. The variable x has a loglogistic distribution with location parameter μ and scale parameter $\sigma > 0$ if $\ln(x)$ has a logistic distribution with parameters μ and σ . The parameters are determined by least square fitting of the probability density values of the hanger's longitudinal and transverse vibration amplitudes based on Eq. (8). Probability density fitting curves of the 1# hanger's longitudinal and transverse vibration amplitudes in each load case based on one year's measured data are shown in Fig. 14, and the corresponding estimated parameter values are shown in Tables 4 and 5 respectively. It can be seen from the figure that:

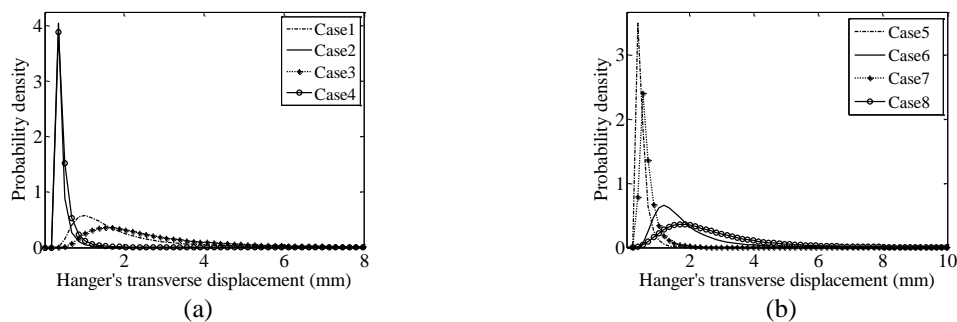


Fig. 13 Probability density fitting curves of the 1# hanger's transverse dynamic displacement amplitudes: (a) for load cases 1~4 and (b) for load cases 5~8

Table 3 Estimated parameter values based on the generalized extreme value distribution function for the 1# hanger's transverse dynamic displacement amplitudes

Load case	1	2	3	4	5	6	7	8
r	0.5355	0.3811	0.4543	0.4237	0.2571	0.3022	0.3155	0.2293
a	0.7167	0.0736	1.1092	0.1025	0.1061	0.5838	0.1560	1.0398
b	1.2608	0.3203	1.9218	0.3824	0.4374	1.3398	0.5679	1.9497

- 1) Here the loglogistic distribution function can describe the probability density distribution characteristics well, which indicates that the 1# hanger's longitudinal and transverse vibration amplitudes in each load case have obvious probabilistic characteristics.
- 2) With the same load, both the longitudinal and transverse vibration amplitudes in the load cases close to the 1# hanger are much smaller than those in the load cases far away from the 1# hanger.
- 3) In the same carriageway, the influence of the load on both the longitudinal and transverse vibration amplitudes is very small. But the influences of the load on both the longitudinal and transverse vibration amplitudes of 1# hanger in load cases 1 and 3 are slightly larger than the others.

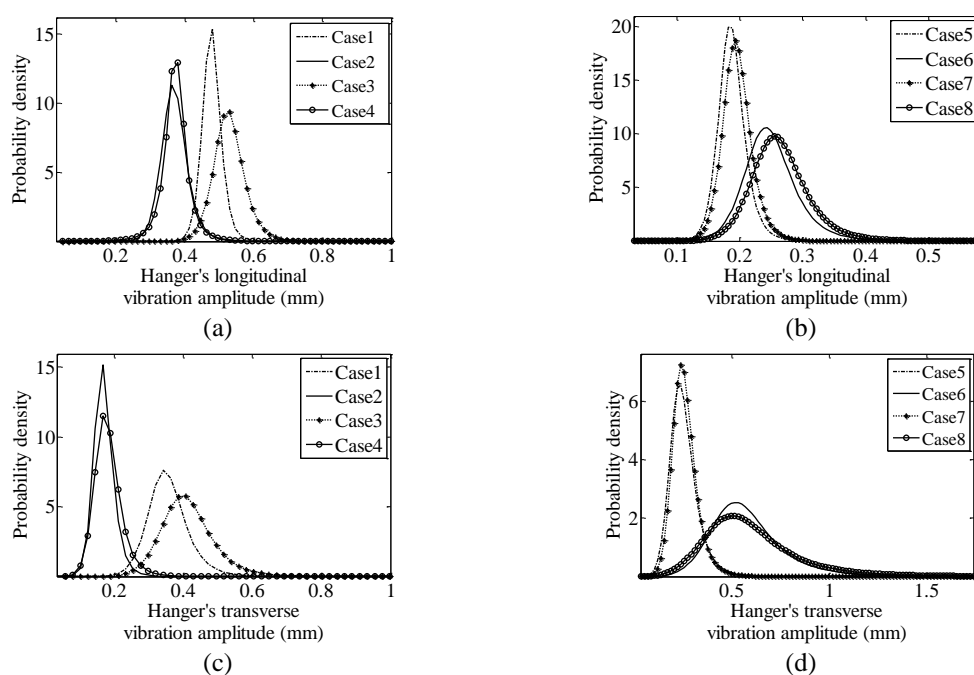


Fig. 14 Probability density fitting curves of the 1# hanger's longitudinal and transverse vibration amplitudes: (a) for the longitudinal vibration amplitudes of load cases 1~4, (b) for the longitudinal vibration amplitudes of load cases 5~8, (c) for the transverse vibration amplitudes of load cases 1~4 and (d) for the transverse vibration amplitudes of load cases 5~8

Table 4 Estimated parameter values of the loglogistic distribution function for the 1# hanger's longitudinal vibration amplitudes

Load case	1	2	3	4	5	6	7	8
μ	-0.7385	-0.9985	-0.6408	-0.9945	-1.6801	-1.4013	-1.6363	-1.3447
σ	0.0337	0.0600	0.0502	0.0653	0.0669	0.0968	0.0692	0.0993

Table 5 Estimated parameter values of the loglogistic distribution function for the 1# hanger’s transverse vibration amplitudes

Load case	1	2	3	4	5	6	7	8
μ	-1.0452	-1.7844	-0.8989	-1.7247	-1.4002	-0.5854	-1.3710	-0.5796
σ	0.0941	0.0985	1.066	0.1215	0.1578	0.1834	0.1382	0.2263

3.1.3 Dynamic load factor

Various probability density functions are used to compare the goodness of fit for the 1# hanger’s longitudinal dynamic load factors in each load case. Finally the t location-scale distribution is selected to describe the probability density statistic characteristics. The parameters are determined by least square fitting of probability density of the 1# hanger’s longitudinal dynamic load factors based on Eq. (6). Probability density fitting curves of the 1# hanger’s longitudinal dynamic load factors in each load case based on one year’s measured data are shown in Fig. 15, and the corresponding estimated parameter values are shown in Table 6. It can be seen from the figure that:

- 1) Here the t location-scale distribution function can describe the probability density distribution characteristics well, which indicates that the 1# hanger’s longitudinal dynamic load factors in each load case have obvious probabilistic characteristics.
- 2) With the same load, the longitudinal dynamic load factors in the load cases close to the 1# hanger are much smaller than those in the load cases far away the 1# hanger.
- 3) In the same carriageway, the 1# hanger’s longitudinal dynamic load factors in load cases with a 16-carriage train are much smaller than those in load cases with a 8-carriage train.

Table 6 Eestimated parameter values of the t location-scale distribution function for the 1# hanger’s longitudinal dynamic load factors

Load case	1	2	3	4	5	6	7	8
μ	1.2178	1.1271	1.1373	1.0751	1.0592	1.1085	1.0395	1.0794
σ	0.0352	0.0172	0.0197	0.0078	0.0076	0.0343	0.0038	0.0021
ν	8.3116	3.1367	7.4968	2.5278	3.0994	13.6060	2.1107	14.5493

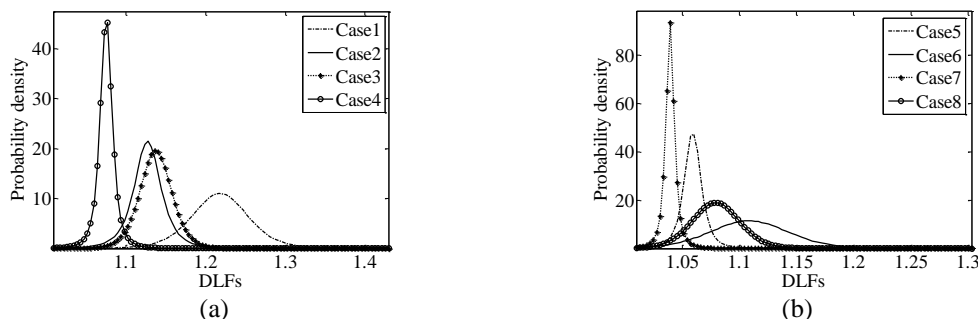


Fig. 15 Probability density fitting curves of the 1# hanger’s longitudinal dynamic load factor for the 8 load cases: (a) for load cases 1~4; (b) for load cases 5~8

Various probability density functions are used to compare the goodness of fit for the 1# hanger's transverse dynamic load factors in each load case; finally the generalized extreme value distribution is selected to describe the probability density distribution characteristics. The parameters are determined by least square fitting of probability density of the 1# hanger's transverse dynamic load factors based on Eq. (7). Probability density fitting curves of the 1# hanger's transverse dynamic load factors in each load case based on one year's measured data are shown in Fig. 16, and the corresponding estimated parameter values are shown in Table 7. It can be seen from the figure that:

- 1) Here the generalized extreme value distribution function can describe the probability density distribution characteristics well, which indicates that the 1# hanger's transverse dynamic load factors in each load case have obvious probabilistic characteristics.
- 2) Different with the 1# hanger's longitudinal dynamic load factors, with the same load, the transverse dynamic load factors in the load cases close to the 1# hanger are much greater than those in the load cases far away from the 1# hanger.
- 3) Different with the 1# hanger's longitudinal dynamic load factors, in the same carriageway, the 1# hanger's transverse dynamic load factors in load cases with a 16-carriage train are slightly smaller than those in load cases with a 8-carriage train.

For the 8 railway load cases, this section gives the probability statistical analysis results for the dynamic displacement amplitudes, the vibration amplitudes and the dynamic load factors, which indicate that the randomness in the hanger vibration is very obvious. Comparisons of the analysis results in each load case with consideration of the carriageway and carriage number are further conducted and some trends are found. This section lays a foundation for further study of probability analysis method for the hanger vibration under the coupled vibration of the train and the bridge.

Table 7 Estimated parameter values based on the generalized extreme value distribution function for the 1# hanger's transverse dynamic load factor

Load case	1	2	3	4	5	6	7	8
r	0.2630	-0.0779	0.2692	-0.0178	-0.1136	0.2163	-0.0483	0.4386
a	0.0763	0.2000	0.0507	0.1763	0.2201	0.1350	0.1542	0.0784
b	1.0878	1.3294	1.0643	1.2531	1.3735	1.1767	1.2351	1.0971

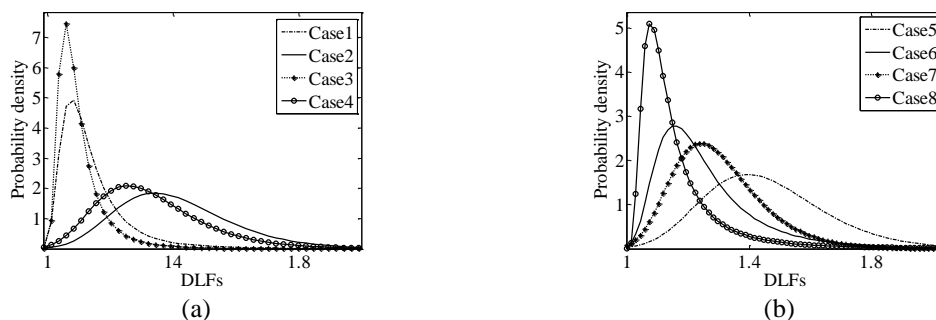


Fig. 16 Probability density fitting curves of the 1# hanger's transverse dynamic load factor for the 8 load cases: (a) for load cases 1~4 and (b) for load cases 5~8

3.2 Coupled vibration characteristics of the hanger and the main girder

Coupled vibration analysis of the hanger and the main girder in the 8 load cases is discussed in detail in this section through the following two points: (1) Hysteretic analysis of the dynamic displacement time histories; (2) Correlation analysis of the vibration amplitudes. Figs. 17 and 18 illustrate the correlation analysis of the 1# hanger's longitudinal and transverse displacements and the main girder's transverse displacements in each load case. It can be seen that: (1) There is good correlation between the 1# hanger's longitudinal and transverse static displacements and the main girder's transverse static displacements in each load case, and their relationships are shown in the hysteresis curves; it can be seen that the deformation capacity of the bridge is very good when the train is running through the bridge; (2) While correlation results between the 1# hanger's longitudinal/transverse dynamic displacement and the main girder's transverse dynamic displacement in each load case fluctuate obviously around the static displacement hysteresis curve. It can be seen from Figs. 17 and 18 that the correlations between the hanger's longitudinal/transverse dynamic displacement and the main girder's transverse dynamic displacement show the phenomenon of hysteresis curves.

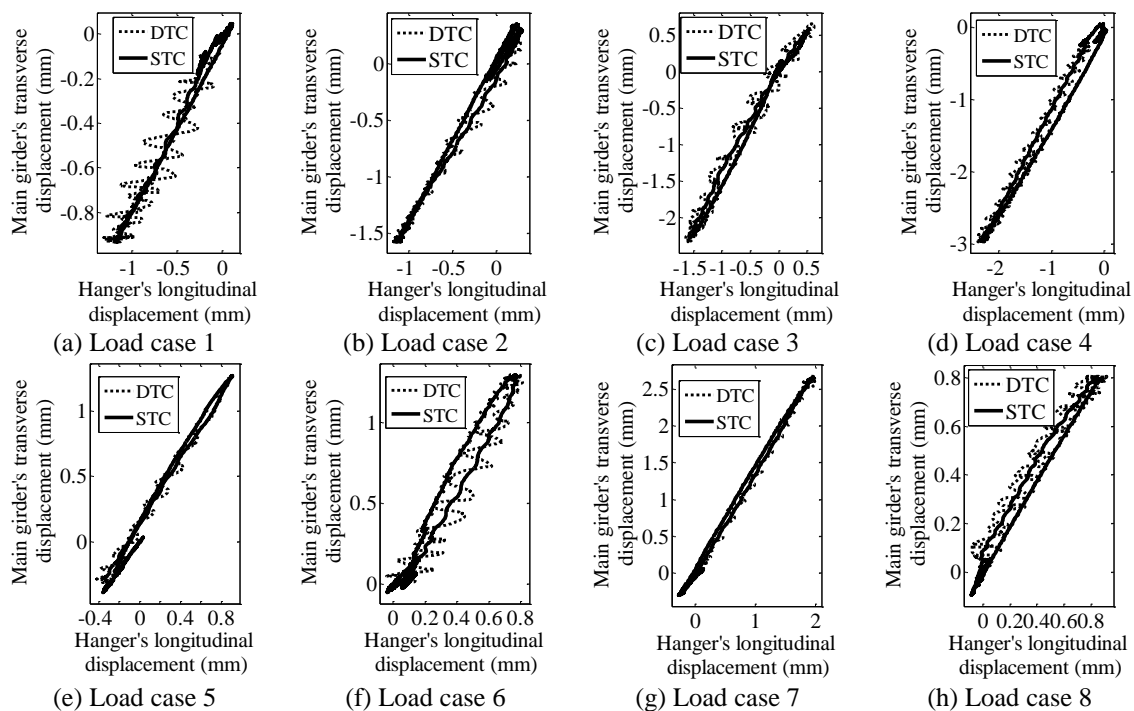


Fig. 17 Correlations between the 1# hanger's longitudinal dynamic/static displacement and the main girder's transverse dynamic/static displacement for every load case (DTC refers to the dynamic displacement time history; STC refers to the static displacement time history)

The possible explanation is as follows: the pass of a train brings the main girder's transverse dynamic displacement, and then brings the hangers' transverse/longitudinal dynamic displacements, which results in the coupled vibration between the train, main girder and hangers; it can be seen from the time history of the hysteresis curves that the values of a hysteresis curve fluctuate slightly around the coordinate (0, 0) before the pass of a train; the hysteresis curves fluctuate in a anticlockwise direction when a train passes through, and the hangers' dynamic displacement continues to increase when the main girder's transverse dynamic displacement increases to its maximum, while the hangers' dynamic displacement increases to its maximum when the main girder's transverse dynamic displacement decreases. Fig. 19 and Fig. 20 show correlation analysis of the 1# hanger's longitudinal/transverse vibration amplitudes and the main girder's transverse vibration amplitudes in load cases 1 and 2 respectively. It can be seen from the two figures that: there is no correlation between the 1# hanger's longitudinal/transverse vibration amplitudes and the main girder's transverse vibration amplitudes. The same conclusion is found in the rest load cases but the results are not shown in detail here. As a result, there is a good correlation between the main girder's static displacement amplitudes and the 1# hanger's static displacement amplitudes; while there is no correlation in their vibration amplitudes. This is because the vibration caused by the train-induced local wind field is another important source for the hanger vibration besides the coupled vibration of the train and the bridge.

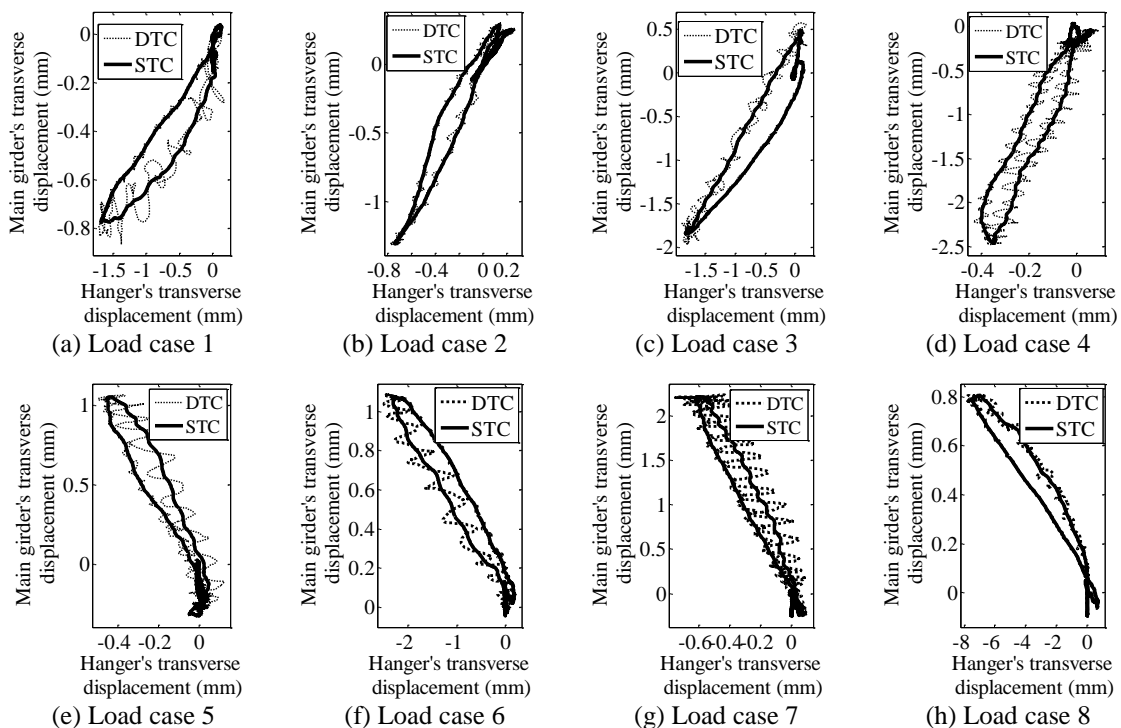


Fig. 18 Correlations between the 1# hanger's transverse dynamic/static displacement and the main girder's transverse dynamic/static displacement for every load case

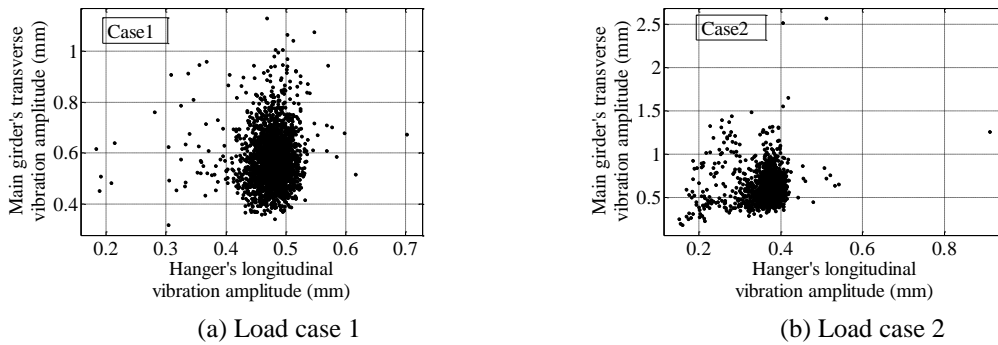


Fig. 19 Correlation results of the 1# hanger's longitudinal vibration amplitudes and the main girder's transverse vibration amplitudes

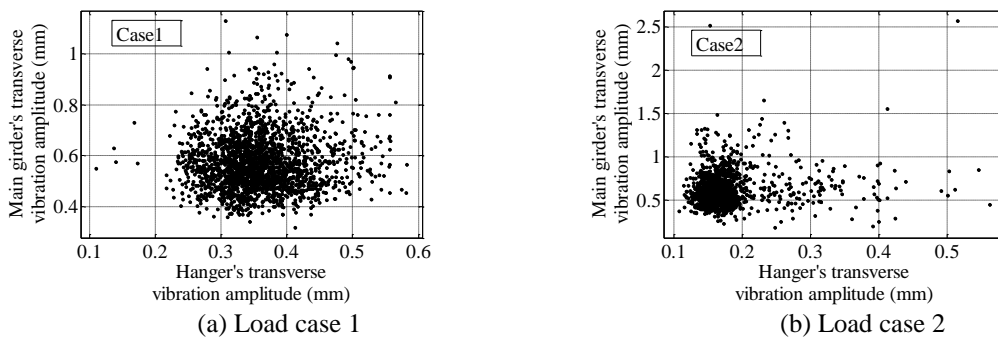


Fig. 20 Correlation results of the 1# hanger's transverse vibration amplitudes and the main girder's transverse vibration amplitudes

4. Conclusions

In this study, an evaluation of train-induced hanger vibration in the Dashengguan Yangtse River Bridge is carried out using the field monitoring data. On the basis of the results obtained from this study, the conclusions that can provide reference for the similar kind of bridges are drawn as follows:

(1) The present work proposes a method to identify the load cases according to the relationship of responses of strain sensors and accelerometers in the SHM system of the bridge, and then the fine analysis of the hanger's vibration characteristics are conducted based on 8 railway load cases.

(2) The hanger's three vibration parameters in each load case, i.e., dynamic displacement amplitude, dynamic load factor and vibration amplitude in the longitudinal and transverse directions respectively, have obvious probabilistic characteristics. However, they fall into different distribution functions.

(3) There is good correlation between the hanger's longitudinal and transverse dynamic displacement and the main girder's transverse dynamic displacement in each load case, and their

relationships are shown in the hysteresis curves. However, there is no correlation between the hanger's vibration amplitudes and the main girder's vibration amplitudes.

(4) With the same load (i.e., the same carriage number), the influences of carriageways on the hanger's three parameters in both longitudinal and transverse directions are different. Transverse dynamic load factors in load cases close to the hanger are much larger than those in load cases far away the hanger; while dynamic displacement amplitudes and vibration amplitudes in both directions, and longitudinal dynamic load factors in load cases close to the hanger are smaller than those in load cases far away the hanger.

(5) Influences of the carriage number on three parameters of the hanger in both longitudinal and transverse directions are different. For bidirectional dynamic displacement amplitudes, their values in load cases with a 16-carriage train are larger than those in load cases with a 8-carriage train; for bidirectional vibration amplitudes, their values in load case 1 are smaller than those in load case 3, but in the other load cases the influences of the carriage number are very small; for bidirectional dynamic load factors, their values in load cases with a 16-carriage train are smaller than those in load cases with a 8-carriage train.

Acknowledgments

The authors gratefully acknowledge the National Basic Research Program of China (973 Program) (2015CB060000), the National Science and Technology Support Program of China (2014BAG07B01), the National Natural Science Foundation (51578138 & 51508070), the Program of "Six Major Talent Summit" Foundation (1105000268), and the Fundamental Research Funds for the Central Universities (DUT16YQ101).

References

- Acampora, A., Macdonald, J.H.G., Georgakis, C.T. and Nikitas, N. (2014), "Identification of aeroelastic forces and static drag coefficients of a twin cable bridge stay from full-scale ambient vibration measurements", *J. Wind Eng. Ind. Aerod.*, **124**, 90-98.
- An, Y.H., Blachowski, B. and Ou, J.P. (2016), "A degree of dispersion-based damage localization method", *Struct. Control Health Monit.*, **23**, 176-192.
- An, Y.H., Ou, J.P., Li, J. and Spencer, B.F. (2014), "Stochastic DLV method for steel truss structures: Simulation and experiment", *Smart Struct. Syst.*, **14**(2), 105-128.
- An, Y.H., Spencer, B.F. and Ou, J.P. (2015), "A test method for damage diagnosis of suspension bridge suspender cables", *Comput. -Aided Civil Infrastruct. E.*, **30**(10), 771-784.
- Antony, S. and Matthew, G.K. (2002), "Modeling duration of urban traffic congestion", *J. Transportation Eng.*, **128**(6), 587-590.
- Bayraktar, A., Altunisik, A.C., Sevim, B. and Turker, T. (2010), "Finite element model updating of Kömürhan Highway Bridge based on experimental measurements", *Smart Struct. Syst.*, **6**(4), 373-388.
- Chatterjee, P.K. and Datta, T.K. (1995), "Dynamic analysis of arch bridges under travelling loads", *Int. J. Solids Struct.*, **32**(11), 1585-1594.
- Chen, Z.Q., Liu, M.G., Hua, X.G. and Mou, T.M. (2011), "Flutter, galloping, and vortex-induced vibrations of H-section hangers", *J. Bridge Eng. - ASCE*, **17**(3), 500-508.
- Chiu, Y.T., Lin, T.K., Hung, H.H., Sung, Y.C. and Chang, K.C. (2014), "Integration of in-situ load experiments and numerical modeling in a long-term bridge monitoring system on a newly-constructed widened section of freeway in Taiwan", *Smart Struct. Syst.*, **13**(6), 1015-1039.

- Ding, Y.L., An, Y.H. and Wang, C. (2015), "Long-term monitoring and analysis of hanger vibration of a high-speed railway steel truss arch bridge", *Proceedings of the 2015 World Congress on Advances in Structural Engineering and Mechanics (ASEM15)*, Incheon, Korea, 25-29 August, 2015.
- Feng, M.Q., Chen, Y.B. and Tan, C.A. (2005), "Global structural condition assessment of highway bridges by ambient vibration monitoring". *Proc. SPIE 5769*, Nondestructive Detection and Measurement for Homeland Security III, 5769, 111-125.
- Ju, S.H. and Lin, H.T. (2003), "Numerical investigation of a steel arch bridge and interaction with high-speed trains", *Eng. Struct.*, **25**(2), 241-250.
- Katani, R. and Shahmorad, S. (2012), "A block by block method with Romberg quadrature for the system of Urysohn type Volterra integral equations", *Eng. Anal. Bound. Elemen.*, **35**(1), 129-139.
- Li, H., Ou, J.P., Zhang, X.G., Pei, M. S. and Li, N. (2015b), "Research and practice of health monitoring for long-span bridges in the mainland of China", *Smart Struct. Syst.*, **15**(3), 555-576.
- Li, J., Hao, H. and Lo, J.V. (2015c), "Structural damage identification with power spectral density transmissibility: numerical and experimental studies", *Smart Struct. Syst.*, **15**(1), 15-40.
- Li, J., Hao, H., Fan, K.Q. and Brownjohn, J. (2015a), "Development and application of a relative displacement sensor for structural health monitoring of composite bridges", *Struct. Control Health Monit.*, **22**(4), 726-742.
- Liu, Z.J., Li, Y.H., Tang, L.Q., Liu, Y.P., Jiang, Z.Y. and Fang, D.N. (2014), "Localized reliability analysis on a large-span rigid frame bridge based on monitored strains from the long-term SHM system", *Smart Struct. Syst.*, **14**(2), 209-224.
- Malm, R. and Andersson, A. (2006), "Field testing and simulation of dynamic properties of a tied arch railway bridge", *Eng. Struct.*, **28**(1), 143-152.
- Ni, Y.Q., Hua, X.G., Wong, K.Y. and Ko, J.M. (2007), "Assessment of bridge expansion joints using long-term displacement and temperature measurement", *J. Perform. Constr. Fac.*, **21**(2), 143-151.
- Ni, Y.Q., Ye, X.W. and Ko, J.M. (2006), "Fatigue reliability analysis of a suspension bridge using long-term monitoring data", *Key Eng. Mater.*, **321-323**, 223-229.
- Norouzi, M., Hunt, V. and Helmicki, A. (2013), "Abnormal behavior detection in the Jeremiah Morrow Bridge based on the long term measurement data patterns". *Proc. SPIE 8695*, Health Monitoring of Structural and Biological Systems 2013, 869536.
- Pinkaew, T. and Senjuntichai, T. (2009), "Fatigue Damage Evaluation of Railway Truss Bridges from Field Strain Measurement", *Adv. Struct. Eng.*, **12**(1), 53-69.
- Saito, T. and Sakata, H. (1999), "Aerodynamic stability of long-span box girder bridges and anti-vibration design considerations", *J. Fluids Struct.*, **13**(7), 999-1016.
- Shao, Y., Sun, Z.G., Chen, Y.F. and Li, H.L. (2015), "Impact effect analysis for hangers of half-through arch bridge by vehicle-bridge coupling", *Struct. Monit. Maint.*, **2**(1), 65-75.
- The Math Works Inc. Statistic Toolbox™ 7 user's guide [R/OL]. 2010. http://www.mathworks.cn/help/releases/R13sp2/pdf_doc/stats/stats.pdf
- Wang, G.X., Ding, Y.L., Song, Y.S., Wu, L.Y., Yue, Q. and Mao, G.H. (2015), "Detection and location of the degraded bearings based on monitoring the longitudinal expansion performance of the main girder of the Dashengguan Yangtze Bridge", *J. Perform. Constr. Fac.*, 04015074.
- Xia, H.W., Ni, Y.Q., Wong, K.Y. and Ko, J.M. (2012), "Reliability-based condition assessment of in-service bridges using mixture distribution models", *Comput. Struct.*, **106**, 204-213.
- Ye, X.W., Ni, Y.Q., Wong, K.Y. and Ko, J.M. (2012), "Statistical analysis of stress spectra for fatigue life assessment of steel bridges with structural health monitoring data", *Eng. Struct.*, **45**, 166-176.
- Zeng, Y. and Tan, H.M. (2012), "Reliability Assessment of Fatigue Life of Hangers in Large-Span Suspension Bridges", *Appl. Mech. Mater.*, **147**, 149-152.
- Zhou, L.R., Yan, G.R., Wang, L. and Ou, J.P. (2013). "Review of benchmark studies and guidelines for structural health monitoring", *Adv. Struct. Eng.*, **16**(7), 1187-1206.